

# Growth Patterns Inferred from Anatomical Records<sup>1</sup>

## Empirical Tests Using Longisections of Roots of *Zea mays* L.

Wendy Kuhn Silk\*, Elizabeth M. Lord, and Kathleen J. Eckard

Department of Land, Air, and Water Resources, University of California, Davis, California 95616 (W.K.S.), and  
Department of Botany and Plant Sciences, University of California, Riverside, California 92521 (E.M.L., K.J.E.)

### ABSTRACT

Our objective was to test whether accurate growth analyses can be obtained from anatomical records and some mathematical formulas. Roots of *Zea mays* L. were grown at one of two temperatures (19°C or 29°C) and were prepared with standard techniques for light microscopy. Positions of cell walls were digitized from micrographs. The digitized data were averaged and smoothed and used in formulas to estimate growth trajectories,  $Z(t)$ , velocities,  $v(z)$ , and strain rates,  $r(z)$ , where  $Z(t)$  is the location occupied by the cellular particle at time  $t$ ; and  $v(z)$  and  $r(z)$  are, respectively, the fields of growth velocity and strain rate. The relationships tested are: for  $Z(t)$ ,  $t = n * c$ ;  $v(z) = l(z) * f$ ; and  $r(z) = f * (\partial/\partial z (l(z)))$ . In the formulas,  $n$  represents the number of cells between the origin and the position  $Z(t)$ ;  $l(z)$  is local cell length; the constant  $c$ , named the 'cellochron,' denotes the time for successive cells to pass a spatial point distal to the meristem;  $f$  is cell flux. Growth trajectories and velocity fields from the anatomical method are in good agreement with earlier analyses based on marking experiments at the two different temperatures. Growth strain rate fields show an unexpected oscillation which may be due to numerical artifacts or to a real oscillation in cell production rate.

For more than three decades, growth physiologists have assumed a consistent model relating patterns of cell length to growth in tissues which have cells that are elongating but not dividing (2, 3, 5, 9-13). The model was inspired by the anatomy of organs with indeterminate growth. In monocot roots, for example, cell division is restricted to an apical region, the meristem, and cell elongation occurs both in the meristem and distally in the 'elongation only' region of the growing organ. Recent theoretical work emphasizes the relationships among growth trajectories, velocity fields, and strain rate fields. These useful quantitative descriptors of growth (8, 9, 18, 21, 25) are usually obtained from time lapse marking experiments of elongating organs. In cases of steady growth (*i.e.* time-invariant fields of velocity and cell production rate), the classical anatomical theories imply that cell length profiles can be used to estimate the growth fields.

If the 'cellochron,'  $c$ , represents the time interval during which a new cell is added to a cell file in the elongation only region, then continuity considerations indicate that during

the cellochron, a more basal cell is displaced from the end of the growth zone (Fig. 1). Figure 1 suggests that  $c$  may be found at any point  $z$  as

$$c = l(z)/v(z) \quad (1)$$

where  $l(z)$  is local cell length, and  $v(z)$  is local velocity. In particular,  $c$  at the base of the elongation zone may be evaluated as the ratio of mature cell length to organ extension rate.

The cell flux,  $f$ , is another useful quantity which is related to the cellochron. Cell flux is the number of cells passing a given point per unit time and can be evaluated from

$$f = v(z)/l(z). \quad (2)$$

Equation 2 shows that  $f$  is the reciprocal of  $c$  and can be computed as the ratio of organ extension rate to mature cell length. The implication of Equation 2 which is relevant to this paper is that local velocity can be evaluated as the product of cell flux and local cell length:

$$v(z) = f * l(z). \quad (2a)$$

A plot of cell length *versus* position can be differentiated to obtain the strain rate,  $r(z)$ :

$$r(z) = \partial v/\partial z = f * (\partial l/\partial z) \quad (3)$$

If growth is steady, then successive cells have similar growth trajectories. Thus for an organ in steady growth, counting cells in a file is equivalent to counting cellochrons of age. Furthermore, according to the model diagrammed in Figure 1, the time required for a cell to move between positions  $z=a$  and  $z=b$  is given by  $c$  times the number of cells between the two positions. Therefore, for the growth trajectory  $Z(t)$ ,

$$t = c * n(Z) \quad (4)$$

where  $n(Z)$  is the number of cells between the origin and the spatial position instantaneously occupied by the cellular particle.

Equations 1 through 4 constitute a mathematical description of the classical model diagrammed in Figure 1 and suggest a method for obtaining growth analyses from anatomical records of organs whose extension rate is known. These relationships have been proposed by different authors. Equation 2a was used by Scott *et al.* (23) to obtain velocities for determinations of ion uptake rates. Gray and Scholes (13) proposed Equation 4 in an analysis of the effects of ionizing radiation. Silk (24) used Equation 3 to obtain strain rate fields

<sup>1</sup> Supported by grants DCB8417504 and DCB8802033 from the National Science Foundation to W. K. S.

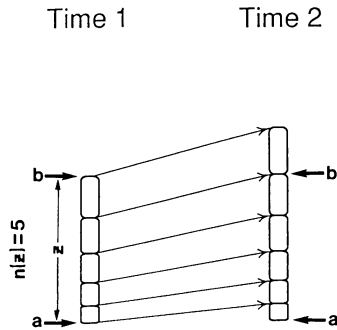


**Figure 1.** Diagram of classical model of cell elongation and displacement. During a cellochron time interval, a small cell is added to the apical end of the file of elongating cells. Each existing cell is presumed to be displaced to the position previously occupied by its distal neighbor in the file. Thus the difference in cell length between neighboring cells should equal the amount of elongation experienced during a cellochron. The time for a tissue particle to move from spatial point  $a$  to point  $b$  should equal the cellochron times  $n(z)$ , the number of cells between the two points.

for organs for which cell length profiles had been published. While this manuscript was in preparation, Gandar and Hall (9) published derivations of these equations as special cases of a more general theory based on the continuity equation and tested versions of Equation 4 with some growth curves in the literature (9). Empirical tests of the model are still rare, however. Here we compare growth analyses based on the anatomical equations to results obtained previously from marking experiments (21) on corn roots grown at 19°C or 29°C.

## MATERIALS AND METHODS

### Plant Material and Anatomical Techniques

Seeds of *Zea mays* L. (cv WF9 × mol7) were germinated and seedlings cultivated in the dark in vermiculite-filled minirhizotrons as previously described (21). After 36 h of growth at 19°C or 17 h at 29°C, when roots were  $5 \pm 0.5$  cm long, the apical 15 mm were excised and fixed in 2.5% glutaraldehyde in 0.025 M phosphate buffer, pH 7.0. After three washes (15 min each) with buffer, samples were dehydrated in ethanol (25%, 50%, 70%; 30 min each) and stored in 70% ethanol at 4°C. The roots were halved into two 7-mm segments while submerged in ethanol, in order to facilitate sectioning. They were then cut at 7 mm, dehydrated to 95% ethanol, infiltrated, and then embedded in glycol methacrylate (JB-4, Polysciences). Serial longisections were cut at 3  $\mu$ m on a Bright 5030 microtome. Sections were stained with toluidine blue O and photographed with Kodak Technical Pan 2415 film (20).

### Cell Length Profiles

Cell files were digitized from 4 × 5 inch negatives (used for the 2–4 mm region) and prints made from 35 mm negatives (used for the 4–14 mm region). Five cortical cell files were identified on each of five roots at 29°C and each of four roots at 19°C (Fig. 2). The cells were mostly contiguous except that, occasionally, when a file became difficult to distinguish on the micrographs, a neighboring file or a similar cortical file on the opposite side of the vascular column was chosen for

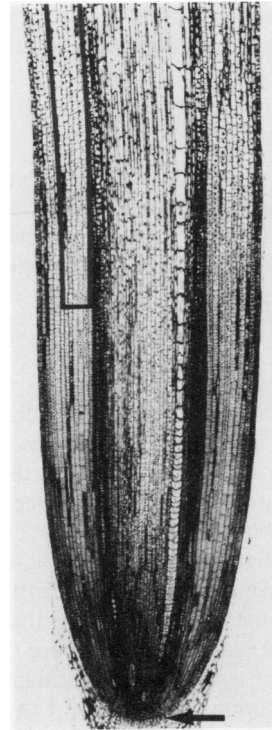


**Figure 2.** Median longisection of a corn root apex. Outline indicates the interior cortical files which were digitized for the analyses of this paper. Arrow indicates origin of coordinate system, 'root apex,' ×67.

digitizing as a continuation of the file. Continuity of the files was always interrupted at the 7-mm location where the root had been cut for section preparation, and so the apical and basal parts of each root needed to be digitized independently. Positions of cell walls were recorded using software written by the senior author for use with a Summagraphics bit pad (MM 1103 series) interfaced with a Zenith microcomputer.

### Numerical Methods

The apex of the root proper (the "root-cap junction" in Barlow's [1] terminology—see Fig. 2) was chosen as origin of the coordinate system. Growth trajectories were obtained by averaging the positions of the basal cell wall for cells of each serial number, with the first serial number assigned to the basal wall found just apical to the 2-mm position. Time corresponding to the serial number  $n$  was computed as  $c \cdot n$ , and the average position,  $z(n)$  was assigned to  $Z(t)$  for use with the formula of Equation 4. Cell length at 0.25-mm increments was obtained by averaging interpolated values from individually splined curves of cell length *versus* position. The spline program was from the International Mathematics and Statistical Library package available on the Davis campus VAX computer and included regression of scattered points and the fitting of splines to knots at 2.0, 4.0, and 6.5 mm in the apical sets of cell files, and to knots at 7.5, 9.5, and 13.0 mm in the distal sets of files. Knots were chosen to fall in the middle of the set of points rather than to anticipate inflection points in the growth curves. The velocity field was obtained using the formula of Equation 2a with the values of average

cell length. Erickson's five point differentiating method (5) was used to evaluate growth strain rates with Equation 3.

## RESULTS

Cell length at any given position is quite variable. A plot of the data for 20 cortical files (from four roots grown at 19°C) shows great scatter (Fig. 3). Mature cortical cell length, for instance, is  $260 \pm 60 \mu\text{m}$  (Table I). And within a single file, cell length does not increase monotonically with position. The interpolating splines smooth rather jagged plots for the individual files (Fig. 4). Analysis of variance confirms that cell length at a given longitudinal position does not differ significantly among roots but does differ with radial position of the cortical file within a root (Table II, see "Discussion").

In spite of the variability in cell length, the average of the interpolated values provides a smoothly increasing function for estimation of the velocity and strain rate fields (Fig. 5). In the apical half of the growth zone, cell length at all locations is independent of temperature. This confirms the conclusion from marking experiments on maize roots that strain (element elongation) is independent of temperature (21). This generalization is only true to a first approximation in the distal third of the growth zone, where cells at the 7.5 to 10-mm locations appear slightly longer in the roots grown at the lower temperature.

Mature cell length is independent of temperature in the range tested (Table I). Thus the cellochron varies only with

elongation rate and decreases from 0.16 h at 19°C to 0.088 h at 29°C (Table I).

Growth trajectories computed from the cell counts and Equation 4 are in good agreement with computations made earlier on the basis of marking experiments (Fig. 6). The velocity fields computed from cell lengths with Equation 2a also are within 15% of the values measured in a 1-h marking experiment (Fig. 7). However, a difference in the shapes of velocity profiles obtained with the two techniques suggests a systematic discrepancy in estimates of the growth strain rate. And indeed, the strain rate fields estimated from cell length data and Equation 3 show a spatial oscillation which does not appear in the curve produced by differentiation of the data from marking experiments (Fig. 8). A trough in the growth rate occurs at both temperatures around 7 mm (where the root was cut) followed by a peak at the 10-mm location. Both of the curves based on anatomical records overestimate the length of the growth zone relative to the curves based on marking experiments. However, the estimates of magnitude and location of maximum strain rate are in good agreement with the marking experiments. The spatial oscillations may be artifacts due to the halving of the 15-mm root during section preparation, or they may originate as oscillations in cell division rate, as explained under "Discussion."

## DISCUSSION

### Historical Context

In both experimental (1, 15, 22) and theoretical (2, 7-9, 14, 18, 19, 24, 25) work of the last decade, careful delineation

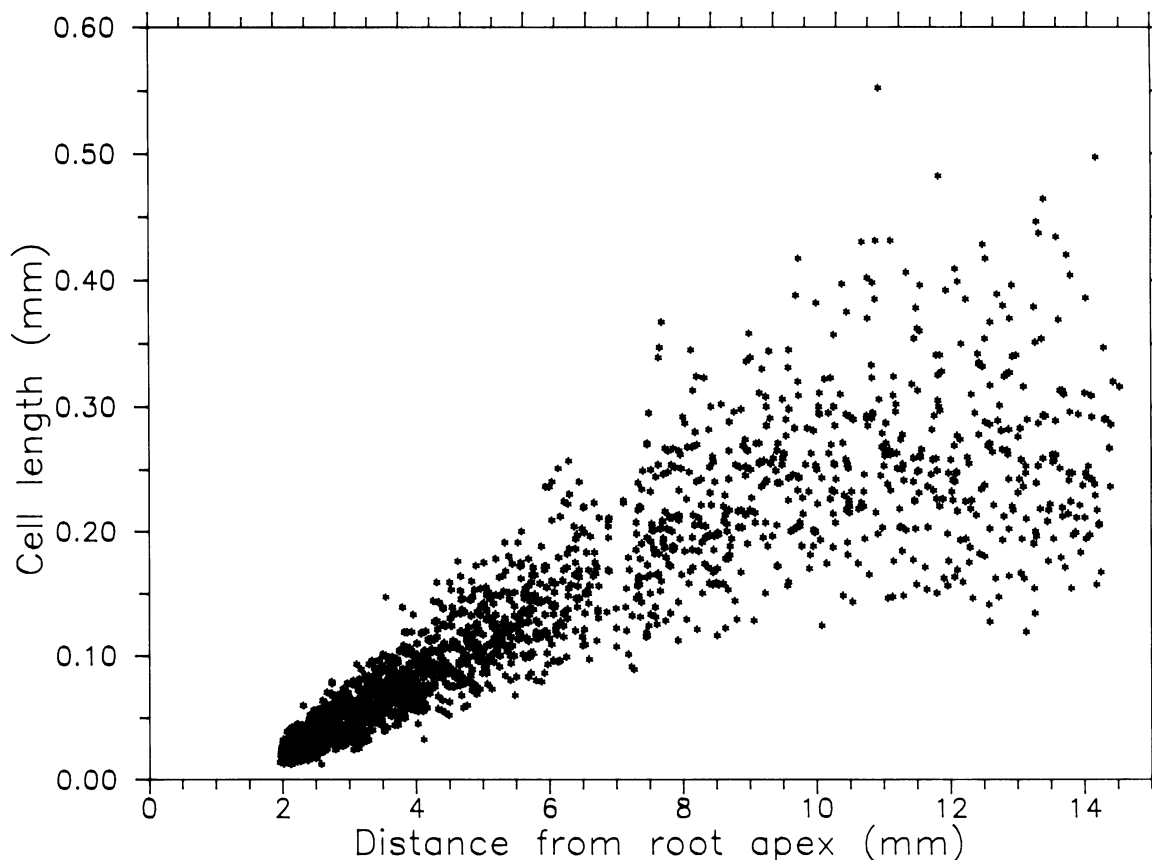
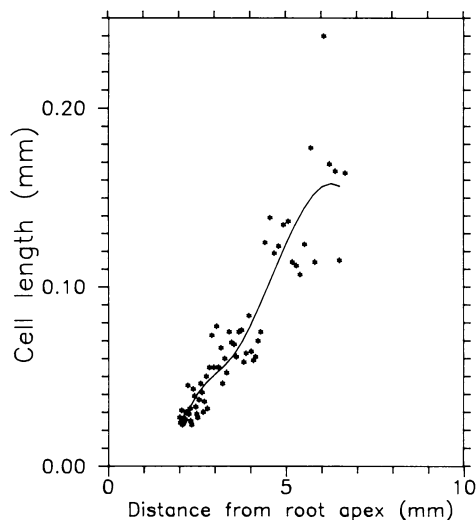


Figure 3. Raw data for 20 cortical files of 4 roots grown at 19°C. Plots of cell length versus position (of apical cell wall) show great scatter.

**Table I.** Mature Cell Lengths, Root Elongation Rates, and Cellochrons

At each temperature, cell lengths are means of >100 cells  $\pm$  SE. Root elongation rates are from (21). The cellochroon is computed as the ratio of mature cell length to root elongation rate.

Temp	Mature Cell Length	Root Elongation Rate	Cellochroon
$^{\circ}\text{C}$	$\mu\text{m}$	$\text{mm h}^{-1}$	$h$
19	$260 \pm 60$	1.62	0.16
29	$265 \pm 57$	3.01	0.088

**Figure 4.** Spline curve through a plot of cell length versus position for a sample cortical file.**Table II.** Analysis of Variance among Files and among Roots

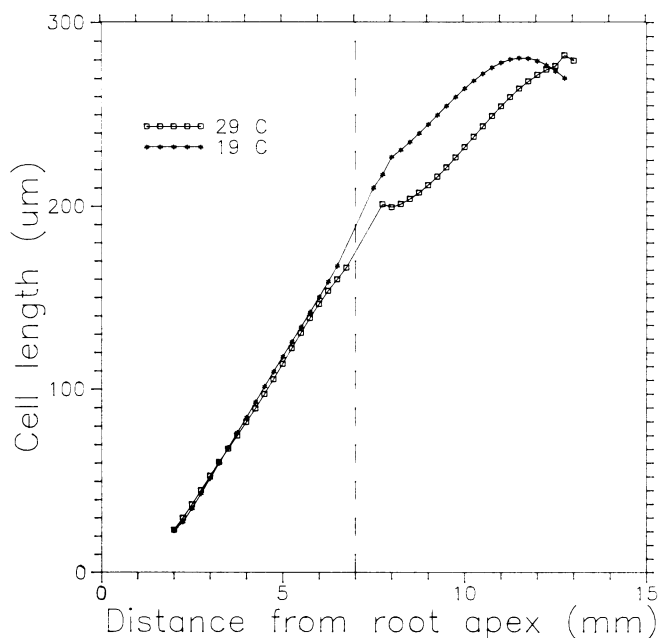
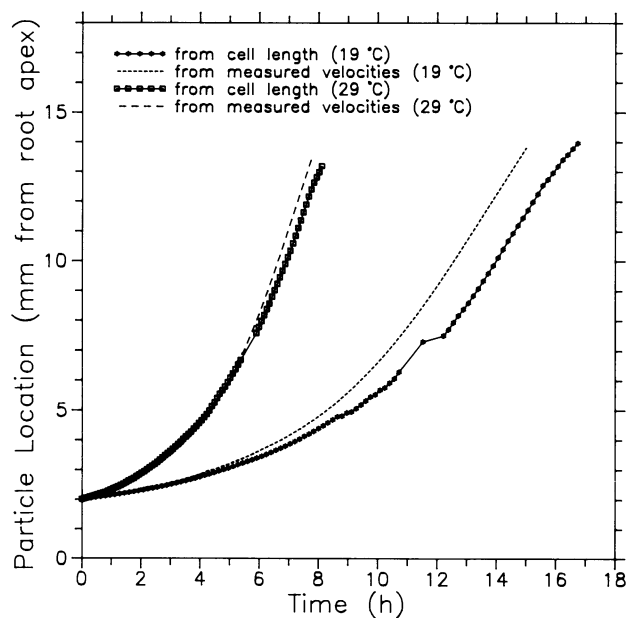
Source of Variation	df	$F_s$
Subgroups	1	
Files	3	5.808***
Roots	2	1.062 NS
Files $\times$ roots	6	4.170***

\*\*\* Significant at 0.01 level; NS, not significant.

of spatial and material aspects of growth has permitted a better understanding of meristem functioning. With some exceptions (12) earlier analyses of cell division patterns were shown to have ambiguities or inaccuracies resulting from omission of either growth strain rates or convective rates of change. Recent analyses, particularly those based on the continuity equation, have clarified relationships among cell size, cell division rate, and cell expansion rate (2, 7–9, 14, 19, 24, 25). In elongation only regions, however (*i.e.* in tissue without cell division), the earlier models seem to be mutually consistent and in agreement with the formalism presented here. Characterization of environmental (3, 10, 13, 27) and genetic (26, 27) effects in terms of growth rate fields, the cellochroon, cell flux, and length of the elongation zone have also used the model tested here.

#### Adequacy of the Model

Tests of the algebraic formulas are also tests of the assumptions of the model. In the model for indeterminate growth,

**Figure 5.** Average cell length as a function of position for roots grown at 19°C (\*) and 29°C (□). For each cortical file (Fig. 4), splines give interpolated values at 0.25-mm increments. The average of the interpolated values gives a smoothly increasing function. Vertical line indicates where root was cut after fixation and prior to sectioning.**Figure 6.** Growth trajectories estimated from cell numbers using Equation 4 compared to estimates from numerical integration of the measured velocity field (from Pahlavanian and Silk [21]). Especially for the 29°C data, the anatomical method is in good agreement with the marking experiments.

cell division is assumed to occur in a localized region, the meristem; cells displaced from the meristem experience elongation as well as displacement until they reach the end of the 'growth zone.' The velocity field is thought to be steady, and the spatial distribution of cell division rates (which produces the cell supply to the elongating file) is also assumed to be steady. These generalizations are perhaps most apt to be valid

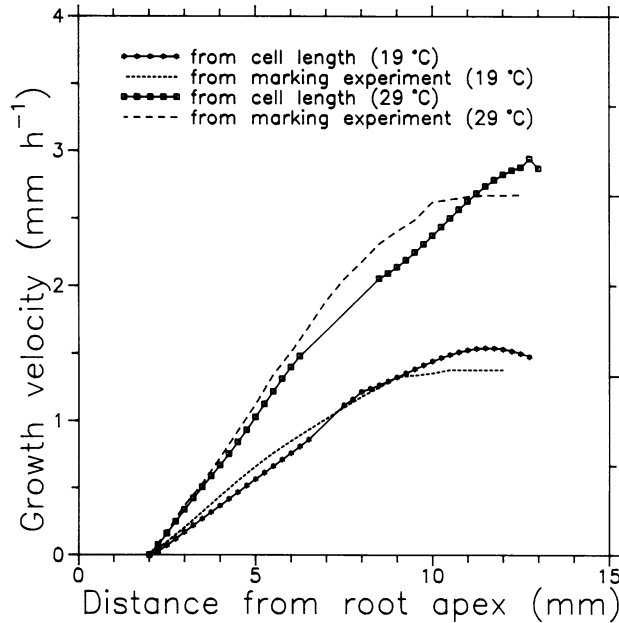


**Figure 7.** Velocity fields estimated from cell lengths with Equation 2a compared to marking experiments (from Pahlavanian and Silk [21]).

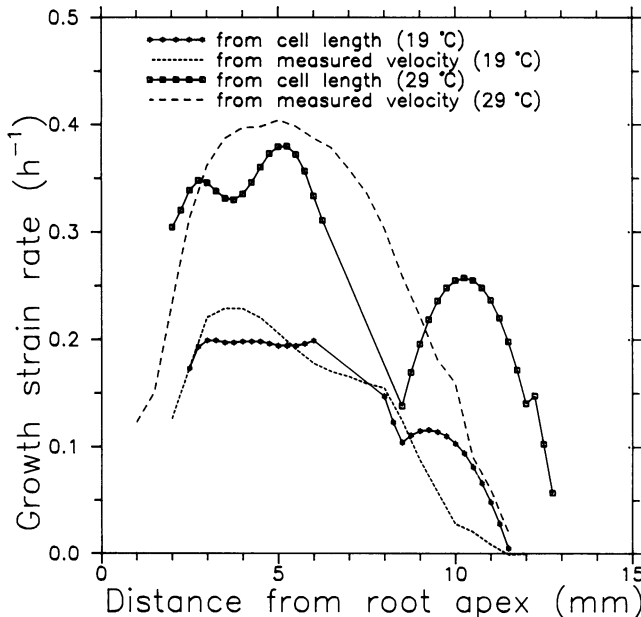


**Figure 8.** Strain rate fields estimated from cell lengths with Equation 3 compared to estimates based on marking experiments (from Pahlavanian and Silk [21]).

for long periods of time in roots of graminaceous plants. In roots of dicotyledonous species, which have less steady growth, the assumptions may be true for shorter periods of time, but for many sets of cells (13, 22, 23). In the grass leaf the basal, intercalary meristem produces most leaf cells and acts for a period like the indeterminate apical meristem of roots. Stem internodes are less suitable for the indeterminate growth model, since spatially periodic patterns of cell length are associated with node placement (6). Organs characterized by nonsteady, determinate growth patterns are not consistent

with the model. Analyses of *Azolla* roots, dicotyledonous leaves, or floral organs, for example, would require time-dependent terms not included in Equations 1 to 4 of this paper. The assumptions of steady fields of growth velocity and cell division rate imply a criterion for suitability of the classical model: The spatial distribution of cell length (cf. Fig. 4) should be invariant with time if the methods of this paper are to be used.

In the maize root there is good empirical evidence for the existence of steady velocity fields (5, 21). There seems to be less evidence for steady cell division patterns, as indicated by the great variability in average cell length at any position (Fig. 3). The variability in average cell length occurs both as a systematic difference among files, and within a file where a cell half or twice the size of its apical neighbor is often encountered. Files in the middle of the cortex have the longest cells; files nearer either the epidermis or the vascular columns have shorter cells (Fig. 2). This is presumed to reflect earlier (more apical) cessation of cell division in the interior layers (17, 28). The presence of an 'extra' cell division just as a cell leaves the meristem is thought to produce the occasional large differences in cell size between adjacent cells within a file (28).

*A priori*, cell trajectories would be expected to have best agreement with the marking experiments, and strain rates would have poorest agreement. This is because counting cell numbers in the file to obtain cell trajectories is, physically, integrating cell formation rates over time. The procedure inherently averages over short-term oscillations in cell division rate. Also, if there is a regular asymmetry in cell division (e.g. if the cell divides into new cells of length  $l$  and  $2l$ ), then this would be averaged in the cumulative cell counts. In contrast, cell length is a local measure; and it is necessary to average over many files before a smoothly increasing spatial distribution can be obtained. Numerical differentiation is a statistically 'noisy' procedure (4); therefore, computation of the strain rate field by differentiating the velocity field is the procedure most subject to error. These *a priori* expectations were met as shown in the good agreement between anatomical and marking methods for growth trajectories and the poor agreement between growth strain rate fields obtained by the two methods. Gandar and Hall (9) also observed good agreement between growth trajectories obtained from anatomical data and those measured or calculated from marking experiments.

The apparent large oscillation in growth strain rate is the least expected result of our tests. The unexpected oscillation could be explained as a biologically real oscillation in cell division rate, or as a numerical artifact. Numerical problems are suggested by the presence of cut ends at the 7-mm position. In general, spline fits are least reliable at the extremes of the data set. And for the cell counts, there is the additional problem that files of longer cells 'drop out' of the data set at earlier serial numbers. For instance, if the middle cortical file had 60 cells between  $z=2$  and  $z=6.5$  mm, an outer file might have 80 cells in the same distance. Thus "average  $z$ " at  $n = 75$  would include only cells from files characterized by smaller cell size. In the distal anatomical sections, the larger cells of the middle cortex would again be included, and  $z$  would appear artificially to increase rapidly with  $n$ . Such effects may have produced the consistent spatial oscillations with a trough

near 7 mm. For future work, randomizing the position where the root is cut for sectioning might minimize this numerical artifact.

Biological interpretations of the apparent spatial oscillation in strain rate are also possible. In onion roots diurnal fluctuations in mitotic index are reported (16). Our procedure included a 10-h interval of darkness between exposures to room light. Exposure to light may trigger a synchronized change in cell division rate, or endogenous mitotic rhythms may occur. Any change in cell division rate relative to growth strain rate will be expressed later in development (when the material tissue element is displaced from the meristem) as a gradient in cell size. If fluctuations in mitotic activity caused the oscillation, then the position of the trough in apparent strain rate would be expected to change with root length (*i.e.* with developmental age). Future anatomical work might be conducted to test this possibility.

### Utility of the Anatomical Method

The anatomical method for inferring growth rate patterns is laborious and time-consuming relative to marking experiments. However, in cases where the marking experiment would perturb the normal growth rate pattern, the anatomical methods would facilitate reasonable estimates of growth patterns. These cases include growth analysis of monocot leaves, where the growing zone is enclosed in a sheath of older leaves, and studies of soil effects on root growth, where marking experiments would have the untenable requirement that the root be visible against a clear surface. Also, anatomical records including contiguous cell files are sometimes collected for other purposes (3, 10, 26, 27); digitizing and analyzing existing anatomical records might prove easier than conducting a separate series of marking experiments.

The results shown here imply that, in cases where steady fields of velocity and cell division rate are thought to occur, the use of Equations 1 through 4 with anatomical records can provide an accurate estimate of growth trajectories and velocity fields and some idea of the strain rate field. These simple equations should not be used, however, when growth is known to be nonsteady, or when environmental fluctuations are expected to perturb spatial distributions of growth velocity or cell division rate.

### LITERATURE CITED

1. Barlow PW (1987) Cellular packets, cell division and morphogenesis in the primary root meristem of *Zea mays* L. *New Phytol* **105**: 27–56
2. Bertaud DS, Gandar PW, Erickson RO, Ollivier AM (1986) A simulation for cell proliferation in root apices. I. Structure of model and comparisons with observed data. *Ann Bot* **58**: 285–301
3. Carmona MA, Cuadrado A (1986) Analysis of growth components in *Allium* roots. *Planta* **168**: 183–189
4. Conte SK, de Boor C (1980) *Elementary Numerical Analysis*, Ed 3. McGraw-Hill, New York
5. Erickson RO, Sax KB (1956) Elemental growth rate of the primary root of *Zea mays*. *Proc Am Philos Soc* **100**: 487–498
6. French JC, Fisher JB (1977) A comparison of meristems and unequal growth of internodes in viny monocotyledons and dicotyledons. *Am J Bot* **64**: 24–32
7. Gandar PW (1980) The analysis of growth and cell production in root apices. *Bot Gaz* **141**: 131–138
8. Gandar PW (1983) Growth in root apices. I. The kinematic description of growth. *Bot Gaz* **144**: 1–10
9. Gandar PW, Hall AJ (1988) Estimating position-time relationships in steady-state, one-dimensional growth zones. *Planta* **175**: 121–129
10. Gonzalez-Bernaldez F, Lopez-Saez JF, Garcia-Ferrera G (1968) Effect of osmotic pressure on root growth, cell cycle and cell elongation. *Protoplasma* **65**: 255–262
11. Goodwin RH, Avers CJ (1956) Studies on roots. III. An analysis of root growth in *Phleum pratense* using photomicrographic records. *Am J Bot* **43**: 479–487
12. Goodwin RH, Stepka W (1945) Growth and differentiation in the root tip of *Phleum pratense*. *Am J Bot* **32**: 36–46
13. Gray LH, Scholes ME (1951) The effect of ionizing radiations on the broad bean root. VIII. Growth rate studies and histological analyses. *Br J Radiol* **24**: 82–92
14. Green PB (1976) Growth and cell pattern formation on an axis. Critique of concepts, terminology and modes of study. *Bot Gaz* **137**: 187–202
15. Gunning BES, Hughes JE, Hardham AR (1978) Formative and proliferative cell divisions, cell differentiation, and developmental changes in the meristem of *Azolla* roots. *Planta* **143**: 121–144
16. Jensen AW, Kavaljian LG (1958) An analysis of cell morphology and the periodicity of division in the root tip of *Allium cepa*. *Am J Bot* **45**: 365–372
17. Luxova M (1975) Some aspects of the differentiation of primary root tissues. In J Torrey, D Clarkson, eds, *The Development and Function of Roots*, Chap. 4. Academic Press, New York, pp 73–90
18. Niklas KJ (1977) Application of finite element analyses to problems in plant morphology. *Ann Bot* **41**: 133–153
19. Niklas KJ, Mauseth JD (1980) Simulation of cell dimensions in shoot apical meristems: implications concerning zonate apices. *Am J Bot* **67**: 715–732
20. O'Brien TP, McCully ME (1981) *The Study of Structure: Principles and Selected Methods*. Termacarpi, Melbourne
21. Pahlavanian A, Silk WK (1988) Effect of temperature on spatial and temporal aspects of growth in the primary maize root. *Plant Physiol* **87**: 529–532
22. Rost TL, Jones TJ, Falk RH (1988) Distribution and relationship of cell division and maturation events in *Pisum sativum* (Fabaceae) seedling roots. *Am J Bot* **75**: 1571–1583
23. Scott BIH, Gulline H, Pallaghy CK (1968) The electrochemical state of cells of the broad bean roots. I. Investigation of elongating roots of young seedlings. *Aust J Biol Sci* **21**: 185–200
24. Silk WK (1984) Quantitative descriptions of development. *Annu Rev Plant Physiol* **35**: 479–518
25. Silk WK, Erickson RO (1979) Kinematics of plant growth. *J Theor Biol* **76**: 481–501
26. Volenec JJ, Nelson CJ (1981) Cell dynamics in leaf meristems of contrasting tall fescue genotypes. *Crop Sci* **21**: 381–385
27. Volenec JJ, Nelson CJ (1983) Responses of tall fescue leaf meristems to N fertilization and harvest frequency. *Crop Sci* **23**: 720–724
28. Webster PL (1980) Analysis of heterogeneity of relative division rates in root apical meristems. *Bot Gaz* **141**: 353–359